BioResearch Open Access
Volume 1, Number 6, December 2012

DOI: 10.1089/biores.2012.0271

A Standardized Rat Model of Volumetric Muscle Loss Injury for the Development of Tissue Engineering Therapies

Xiaowu Wu,[1,2] Benjamin T. Corona,[1] Xiaoyu Chen,[1,3] and Thomas J. Walters[1]

Abstract

Soft tissue injuries involving volumetric muscle loss (VML) are defined as the traumatic or surgical loss of skeletal muscle with resultant functional impairment and represent a challenging clinical problem for both military and civilian medicine. In response, a variety of tissue engineering and regenerative medicine treatments are under preclinical development. A wide variety of animal models are being used, all with critical limitations. The objective of this study was to develop a model of VML that was reproducible and technically uncomplicated to provide a standardized platform for the development of tissue engineering and regenerative medicine solutions to VML repair. A rat model of VML involving excision of ~20% of the muscle's mass from the superficial portion of the middle third of the tibialis anterior (TA) muscle was developed and was functionally characterized. The contralateral TA muscle served as the uninjured control. Additionally, uninjured age-matched control rats were also tested to determine the effect of VML on the contralateral limb. TA muscles were assessed at 2 and 4 months postinjury. VML muscles weighed 22.7% and 19.5% less than contralateral muscles at 2 and 4 months postinjury, respectively. These differences were accompanied by a reduction in peak isometric tetanic force (P_o) of 28.4% and 32.5% at 2 and 4 months. Importantly, P_o corrected for differences in body weight and muscle wet weights were similar between contralateral and age-matched control muscles, indicating that VML did not have a significant impact on the contralateral limb. Lastly, repair of the injury with a biological scaffold resulted in rapid vascularization and integration with the wound. The technical simplicity, reliability, and clinical relevance of the VML model developed in this study make it ideal as a standard model for the development of tissue engineering solutions for VML.

Key words: extracellular matrix; fibrosis; muscle injury; muscle regeneration; regenerative medicine; tissue engineering

Introduction

Volumetric muscle loss (VML) is defined as the traumatic or surgical loss of skeletal muscle with resultant functional impairment.[1] VML represents a challenging clinical problem for both military and civilian medicine.[2,3] Militarily, VML occurs primarily from penetrating soft tissue injuries as a result of explosions[4] and as a consequence of excision and debridement of devitalized muscle tissue following extremity compartment syndrome. In civilian medicine, VML is often associated with penetrating trauma from bullet wounds and motor vehicle accidents. In addition to extremity injuries, craniomaxillofacial trauma is common on the battlefield[5] and in civilian trauma,[6] often involving the loss of soft tissue, including skeletal muscle. In all cases, VML results in severe cosmetic deformities and debilitating functional loss.[1,7]

Surgically, the current standard of care for VML is autologous tissue transfer (muscle flaps) and physical therapy. Nonfunctional muscle flaps are routinely used to provide bony coverage,[8] and there are recent reports describing functional free muscle transplantation in the forearm,[9] elbow,[10] and lower extremities.[11] However, these highly technical procedures are associated with significant donor site morbidity, particularly in the case of large VML in the lower extremities, which relies on other large muscles as donor tissue.[11] Nonsurgical solutions consist primarily of advanced bracing, including advanced energy storing orthoses,[1,12,13] but these solutions are currently limited to VML below the knee.

The treatment limitations for VML repair have been recognized by the military medical community.[1] In response, a variety of tissue engineering and regenerative medicine treatments for VML injury are under preclinical development.[14–18] Currently these therapies are being developed in

[1]Extremity Trauma and Regenerative Medicine Research Program, United States Army Institute of Surgical Research, Fort Sam Houston, Texas.
[2]Department of Surgery, University of Texas Health Science Center, San Antonio, Texas.
[3]Wake Forest Institute for Regenerative Medicine, Winston-Salem, North Carolina.

Report Documentation Page

Form Approved
OMB No. 0704-0188

1. REPORT DATE	2. REPORT TYPE	3. DATES COVERED
01 DEC 2012	**N/A**	**-**

4. TITLE AND SUBTITLE	5a. CONTRACT NUMBER
A standardized rat model of volumetric muscle loss injury for the development of tissue engineering therapies	5b. GRANT NUMBER
	5c. PROGRAM ELEMENT NUMBER
6. AUTHOR(S)	5d. PROJECT NUMBER
Wu X., Corona B. T., Chen X., Walters T. J.,	5e. TASK NUMBER
	5f. WORK UNIT NUMBER
7. PERFORMING ORGANIZATION NAME(S) AND ADDRESS(ES)	8. PERFORMING ORGANIZATION REPORT NUMBER
United States Army Institute of Surgical Research, JBSA Fort Sam Houston, TX	
9. SPONSORING/MONITORING AGENCY NAME(S) AND ADDRESS(ES)	10. SPONSOR/MONITOR'S ACRONYM(S)
	11. SPONSOR/MONITOR'S REPORT NUMBER(S)

12. DISTRIBUTION/AVAILABILITY STATEMENT
Approved for public release, distribution unlimited

13. SUPPLEMENTARY NOTES

14. ABSTRACT

15. SUBJECT TERMS

16. SECURITY CLASSIFICATION OF:			17. LIMITATION OF ABSTRACT	18. NUMBER OF PAGES	19a. NAME OF RESPONSIBLE PERSON
a. REPORT	b. ABSTRACT	c. THIS PAGE			
unclassified	**unclassified**	**unclassified**	**UU**	**11**	

a variety of species and in different muscles including murine lattissumus dorsi muscle,[18] murine tibialis anterior,[19] murine thigh muscle,[20] rat lateral gastrocnemius,[15] rat rectus abdominus muscle,[16] rat thigh muscle,[21] and canine gastrocnemius muscle and achilles tendon.[17] However, the high cost, technical complications, and/or the inability to perform reliable functional assessments limits the interpretation or reproduction of the important findings currently made in this emerging and promising field. Additionally, the lack of a standardized model precludes meaningful comparisons among potential treatments within and across laboratories.

What is needed is a clinically relevant animal model of VML injury that is reliable and technically simple to perform. Foremost, the model needs to involve an injury severity beyond the self-regenerating capacity of the muscle, which is in stark contrast to a number of rodent muscle injury models that damage the musculature using mechanical (e.g., lengthening contractions),[22] chemical (e.g., toxins),[23] or thermal (e.g., cryo-injury)[24] insults. Equally paramount is the ability to perform a standard and reliable functional assessment of the injured muscle or muscle unit. Moreover, given the magnitude of biological regeneration that must occur, current tissue engineering and regenerative medicine treatments for VML are slow healing, requiring many months before measurable improvement in outcomes can be assessed.[16,17] Therefore, it is critical that the model is capable of supporting long-term studies. During this time, the untreated injury should be functionally stable and with low variability. It must lend itself to clinically relevant repair methods. That is to say that methods used to implant and secure the test article should closely approximate those required for clinical application.

The purpose of the current study was to develop a rat model of VML injury that meets these requirements. VML injury was surgically created with a partial excision of the tibialis anterior (TA) muscle in male Lewis rats. Herein we provide a detailed description of the surgical creation of this injury and the irrecoverable functional deficits that ensued over the following 4 months postinjury. Moreover, an example of surgical repair of the VML injury using decellularized muscle extracellular matrix (ECM) is presented. Based on the results of this study, this VML injury model can be used as a standard platform for testing tissue engineering and regenerative medicine approaches for the repair of VML injury.

Materials and Methods

Animals

This study was conducted in compliance with the Animal Welfare Act and the Implementing Animal Welfare Regulations and in accordance with the principles of the Guide for the Care and Use of Laboratory Animals. All animal procedures were approved by the United States Army Institute of Surgical Research Animal Care and Use Committee. Adult male Lewis rats weighing about 350 g at the time of surgery (Harlan Laboratories, Indianapolis, IN) were housed (12-hour light–dark cycle) in a vivarium accredited by the American Association for the Accreditation of Laboratory Animal Care and provided with food and water *ad libitum*.

Anesthesia

All surgical and mechanical testing procedures were carried out under anesthesia with continuous inhalation of isoflurane (1.5–3%). The depth of anesthesia was monitored throughout the experiment by noting the absence or presence of a response to a light toe pinch with hemostats; lack of response was considered a surgical plane of anesthesia and the concentration of isoflurane was adjusted accordingly. Core temperature was monitored using a thermistor and maintained at 36.5–37.5°C by manually adjusting the temperature of water perfusing the surgical bed.

Analgesia

Rats were administered buprenorphine (0.1 mg/kg, subcutaneously) 30 min before and at least every 12 h thereafter for the first 24 h postsurgery. Animal pain and distress were assessed daily by a qualified member of the veterinary staff for the first 2 weeks postsurgery to determine the need for any additional analgesia; no animal required additional analgesia after the first 24 h postsurgery.

TA muscle VML model

The surgical procedure for creating VML in the rat TA muscle is depicted in Fig. 1. Using aseptic technique, a longitudinal incision was made along the lateral aspect of the lower leg using a scalpel (size 11 [BD Bard-Parker™]; Fig. 1A, 1B). The skin was separated from the fascia by blunt dissection. A longitudinal incision was made along the lateral aspect of the fascia covering the TA muscle. The fascia was then bluntly but gently separated from the TA muscle, taking care to keep the fascia intact for later repair (Fig. 1C). With the TA muscle exposed, a micrometer was used to measure distally 1 cm from the proximal origin of the TA muscle (using the tibial tuberosity as a bony landmark). The length of the TA muscle with the foot plantarflexed commonly measured ~30 mm. Using a sterile skin marker, a horizontal line to the long-axis of the muscle was drawn 10 mm from the origin and a second horizontal line was drawn 10 mm below the first line—the middle third of the TA muscle was used to create the TA muscle defect (Fig. 1D). Then, at the demarcated middle third the TA muscle, the TA and extensor digitorum longus (EDL) muscles were bluntly separated and the medial aspect of the TA muscle was separated from the tibia using blunt medium-sized hemostats. A flat spatula was then inserted under the TA muscle (but over the EDL), which flattened the TA muscle in preparation for the creation of the surgical defect (Fig. 1E).

The surgical defect was created by scoring the TA muscle with the dimensions of the defect using a sterile scalpel (size 11). First, two horizontal incisions were made in the TA muscle along the superior and inferior horizontal lines drawn on the muscle (Fig. 1F). The horizontal incisions approximated a third to a half of the depth of the muscle and were not made deeper to avoid damage of the distal tendon; it is advised to start with a smaller defect as revision can be made as necessary. Then, two longitudinal incisions were made on each side of the TA muscle approximately 2–3 mm from the medial and lateral margins of the muscle; the width of the defect was ~7 mm wide. Using forceps to grip the superficial aspect of the proximal portion of the scored area, the defect was then created by reflecting tissue in the scored area from the remaining TA muscle mass using a scalpel (size 11; Fig. 1G). The excised defect was then blotted and weighed, with more tissue in the middle third of the muscle removed until the total defect weight approximated ~20%

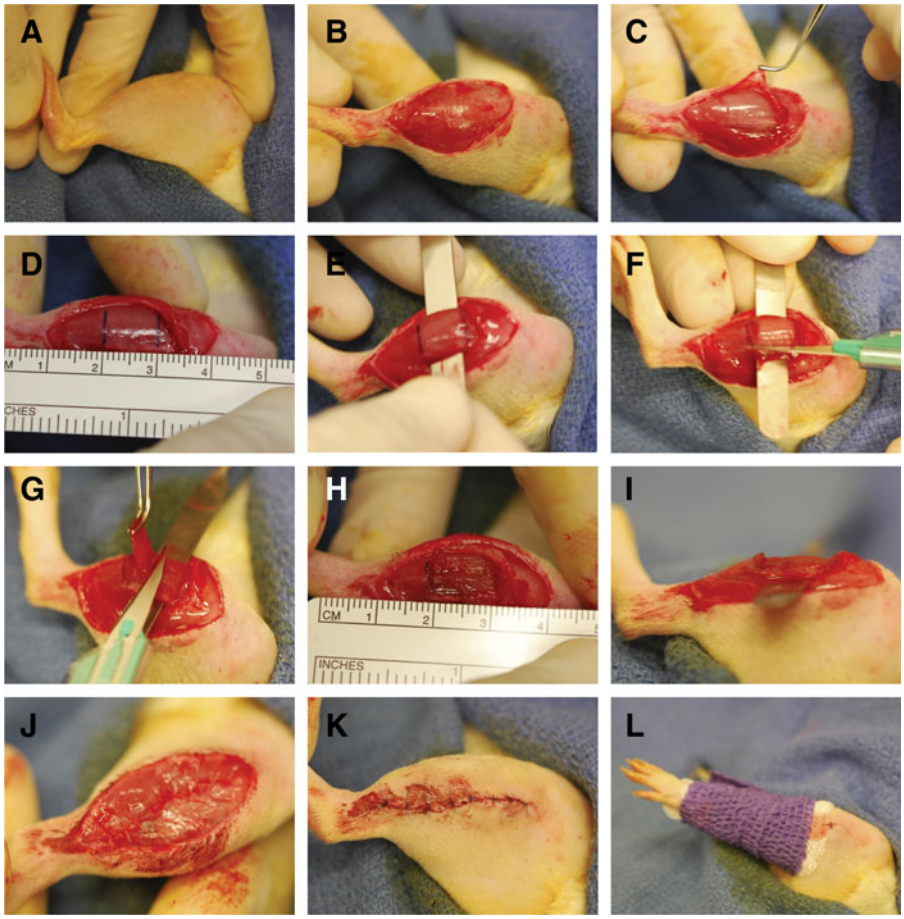

FIG. 1. Illustration of rat tibialis anterior (TA) muscle surgical procedure. Approximately 20% of the rat TA muscle was excised to create an endogenously irrecoverable VML injury. See Materials and Methods for a description of panels **(A–L)**.

of the estimated TA muscle weight (see below). Once the appropriate defect weight is achieved the spatula was removed. The defect dimensions following spatula removal approximated 10 mm × 7 mm × 3 mm (length × width × depth; Fig. 1H, 1I). Prolene (6-0) markers were placed at the corners and margins of the defect to track the area of the defect at the time of harvest. The fascia and skin were closed using vicryl (6-0) and prolene (6-0) interrupted sutures, respectively (Fig. 1J, 1K). A compression bandage was then wrapped around the lower leg for 5–10 min.

During initial model development, we removed progressively larger amounts of muscle tissue followed by a measurement of maximal isometric force (P_o). The final model, and that which all of the subsequent studies are based on, involved a defect corresponding to 20% of the total weight of the TA, which was the largest defect possible that ensured that entry of major blood vessels or nerves at the proximal deep portion of the TA muscle without damaging the distal tendon. To determine the requisite weight of tissue to excise, TA weight was estimated based on the relationship between the weight of the TA and body weight, which was described by the following regression equation: $y = 0.0017 \times \text{body wt.} - 0.0716$ (Supplementary Fig. S2). This formula was based on historical data from our lab for rats of the same sex, strain, and age. The measured TA muscle defect weight was 105 ± 2 mg and 101 ± 1 mg of tissue in the 2-month and 4-month groups, respectively.

Surgical repair of TA muscle with VML

VML repair was performed using rat acellular muscle matrix (RAMM). Immediately after the creation of the muscle defect, RAMM was cut to fit the defect and placed into the defected area and sutured to the remaining TA muscle at the corners and margins of the implant using prolene suture (6-0). Care was taken to include the epimysium of the TA muscle in the suture because this suturing method withstands tension well and thus promotes superior suture retention.[25] Additionally, these sutures were used as markers of the defect–implant interface at the time of harvest. The fascia and skin were closed as previously described.

In situ *mechanical properties*

In situ muscle mechanical properties were measured as previously described.[26,27] The transected common peroneal nerve was stimulated via a nerve cuff electrode using a pulse stimulator (A-M Systems, Inc, Mod. 2100). The distal tendon of the TA was isolated and cut the distal one-third of the TA was dissected free from the surrounding musculature, leaving the origin and neurovascular pedicle intact. The distal tendon was threaded through a hole in the lever arm of a dual-mode servo muscle lever system (Aurora Scientific, Inc., Mod. 309b) and secured with 4-0 silk suture. The lower leg was secured and stabilized with pins at the knee and ankle joints. The temperature of the peroneus longus muscle

was monitored with a needle thermistor and acted as a surrogate for the TA and maintained at 35 ± 1°C. Muscles were set at optimal length (L_o) and all measurements were made using a 100-μsec pulse at a voltage corresponding to 1.5–2 times the voltage required for peak twitch tension (P_t). L_o was determined from P_t using an automated routine as follows: starting in a slack position the muscle was stimulated at 1 Hz for a set of eight twitches; the last two twitches were averaged and the P_t was stored. The lever then automatically moved 0.1 mm, and the routine was repeated 2 sec later. Each twitch set including lever movement took 10 sec. This continued until the average P_t did not change by more than 2% between three consecutive twitch sets, indicating the plateau of the isometric length–tension curve. L_o was defined as the second of the three twitch sets. Following establishment of L_o, peak isometric contractile force was measured with a 300-ms train over a range of frequencies (1–200 Hz). A custom, LabView™ (National Instruments Inc.) based program was used to control the muscle lever systems and collect, store, and analyze the data from *in vivo* and *in situ* muscle function studies.

In vivo *mechanical properties*

Anterior crural muscle *in vivo* mechanical properties were measured in anesthetized rats (isoflurane 2–2.5%) in both legs, with and without EDL muscle distal tenotomy. Core body temperature was monitored and maintained at 36–37°C. For each leg, mechanical properties were determined first with the anterior crural muscles undisturbed. Then, a skin incision was made at the antero-lateral aspect of the ankle, and the distal EDL muscle tendon was isolated and severed above the retinaculum. The TA muscle and tendon as well as the retinaculum were undisturbed. *In vivo* functional measurements were performed using methodology, similar to that we have described previously for mice and rats.[28,29] A nerve cuff was implanted in each leg around the peroneal nerve. The foot was strapped using silk surgical tape to a foot plate attached to a dual-mode muscle lever system (Aurora Scientific, Inc., Mod. 305b). The knee was secured on either side using a custom-made mounting system, and the knee and ankle were positioned at right angles. Peak isometric torque was determined by stimulating the peroneal nerve using a Grass stimulator (S88) at 150 Hz with a pulse-width of 0.1 msec across a range of voltages (2–8 V).

TA muscle decellularization and characterization

TA muscles were isolated from donor Lewis rats and decellularized as previously described[30] with some modifications. Briefly, TA muscles were freeze-thawed and soaked in dH_2O for 72 h, then treated with 0.15% tryspin in Dulbecco's modified Eagle's medium (DMEM; Invitrogen) at room temperature for 2 h. The muscles where then neutralized with 10% fetal bovine serum in DMEM at 4°C overnight, and treated with 3% Triton x-100 (Fisher Scientific) solution till the tissue was clear. The remaining Triton x-100 was then rinsed off with phosphate-buffered saline (PBS). The decellularization was confirmed by histology using hematoxylin and eosin (HE), Masson's Trichrome, and DAPI stains. All RAMM were sterilized with UV light for a minimum of 4 h prior to implantation.

India ink perfusion and tissue processing

Three, 7, 14, and 28 days post–RAMM implantation ($n = 4$ per time point), animals were euthanized and half were perfused with India ink. The TA muscle was isolated and frozen in isopentane submerged in liquid nitrogen for histological analysis.

Histology

Muscles prepared for longitudinal sectioning were fixed in 10% neutral buffered formalin and stored in 60% ethanol, followed by paraffin embedding using a tissue processor (ASP300S, Leica Microsystems). Twelve-micrometer sections were cut and stained with HE and Masson's trichrome. Muscles prepared for cross-sectioning were frozen in 2-methylbutane (isopentane, Fisher 03551-4) supercooled in liquid nitrogen. Cryostat cross-sections (8 μm) were cut from the midsection of the defected area. Sections were stained with HE and Masson's trichrome. Immunofluorescence stained tissue sections were probed for collagen I (1:500, Millipore AB755P), von Willebrand factor (vWF: 1:200, Millipore AB7356), sarcomeric myosin (MF20: 1:10, Hybridoma Bank), laminin (1:200, Abcam AB11575), CD68 (1:50, AbD Serotec MCA341R), cellular membranes (wheat germ agglutinin; WG: 1:20, Invitrogen), and nuclei (DAPI; 1:100, Invitrogen). Sections were blocked in PBS containing 0.05% Tween 20, 5% goat serum, and 0.1% bovine serum for 1 h at room temperature and then incubated in primary antibody solutions overnight at 4°C. Sections were washed in PBS and incubated in corresponding Alexafluor 488 or 596 labeled secondary antibodies (1:200–1:500), Invitrogen) at room temperature for 1 h. The sections were then stained with DAPI and mounted in Fluoromount (Fisher Scientific).

Statistical analyses

SPSS software (SPSS Inc.) was used for all statistic analyses. A paired *t*-test was used to determine differences between the injured and uninjured contralateral control muscle. An unpaired *t*-test was used to compare the uninjured contralateral control muscles to muscles from age-matched control animals. Two-way ANOVA followed by Bonferroni *post hoc* analysis was used to determine differences among ECM size under different decellularization conditions. Difference were considered significant when $p < 0.05$. All values are presented as mean ± standard error of the mean (SEM).

Results

Development of an irrecoverable rat TA muscle VML injury

Preliminary studies. Due the invasive nature of this surgical procedure, preliminary studies were performed to determine the effect of a sham operation on the histological and functional characteristics of the TA muscle. These results are presented in Supplementary Fig. S1. Ultimately, the sham surgery did not alter functional capacity of the anterior crural muscles at 1 month postinjury.

Body weight. At all time points, the body weights for age-matched uninjured control rats were significantly less than VML rats. The body weights of all groups underwent similar increases over the 4 months of the study, with the most rapid

Table 1. Morphological and *In Situ* Tibialis Anterior Muscle Functional Characteristics

	2 months			*4 months*		
	Control (n=3)	*Contra* (n=5)	*VML* (n=5)	*Control* (n=3)	*Contra* (n=9)	*VML* (n=9)
BW (g)						
Pre	320±3[a]	—	349±5	318±5	—	343±3
Final	456±10	—	478±18	475±13	—	490±15
MW						
TA (mg)	646±19[a]	717±30	571±50[b]	766±13	770±41	633±40[b]
TA/BW (mg/g)	1.49±0.07	1.49±0.05	1.19±0.09[b]	1.59±0.02	1.56±0.6	1.29±0.11[b]
EDL (mg)	179±2	193±7	222±12[b]	178±10	200±15	233±22
EDL/TA	27.3±0.5	26.6±1.0	39.3±2.3	23.7±0.6	25.8±1.7	37.0±4.8[b]
TA-P_o						
N	10.7±1.1	11.9±0.7	9.0±0.9[b]	12.1±1.3	12.8±1.3	9.2±1.8[b]
N/g of MW	16.7±1.2	16.9±0.3	16.1±1.6	16.3±1.73	16.7±1.7	14.6±2.7
mN/kg of BW	24.9±1.6	23.9±1.5	18.7±0.6[b]	25.6±1.8	25.9±2.4	18.8±3.4[b]

All values are mean±standard deviation.
[a]Significantly different from VML ($p<0.05$).
[b]Significantly different from contralateral control (Contra) ($p<0.05$).
VML, volumetric muscle loss; BW, body weight; MW, muscle weight; TA, tibialis anterior; EDL, extensor digitorum longus; P_o, peak isometric torque.

increase over the first 2 months. Compared to pre-injury body weight, age-matched control and VML injured groups had increased body weights ranging from 31.4% to 39.6% ($p<0.05$) and only 2.3–4.5% over the initial and final 2 months, respectively (Table 1).

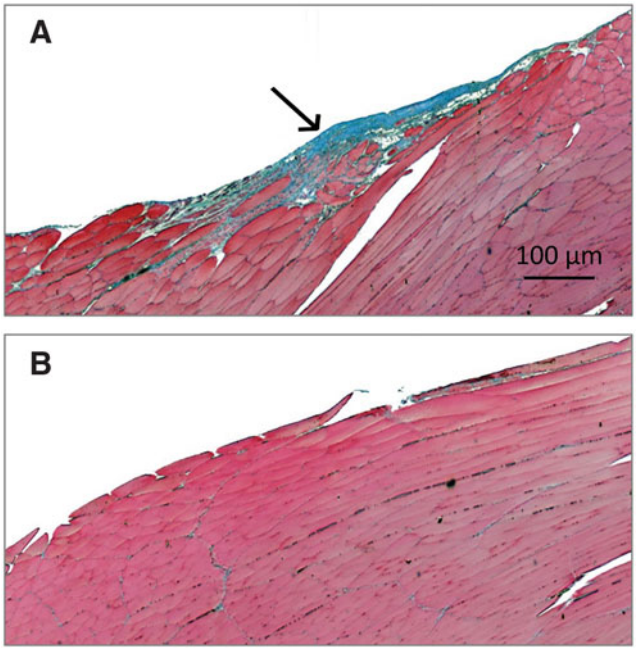

FIG. 2. Longitudinal section of volumetric muscle loss (VML) injured **(A)** and uninjured contralateral control **(B)** (10×) with Masson's Trichrome stain at 2 months postinjury. A thin layer of connective tissue can be seen at the injury site indicative of fibrotic scarring. A number of disorganized muscle cells were present within or in the immediate vicinity of the wound site.

TA and EDL muscle weight

In the VML groups, the TA weight was 20.4% and 17.8% less than the contralateral uninjured muscles 2 and 4 months postinjury, indicating that the injured muscle did not appreciably regenerate during this time. EDL muscles from VML injured legs weighed 13.1% and 14.2% more at 2 and 4 months postinjury, than those from the contralateral control leg, indicating that VML resulted in compensatory hypertrophy of synergist muscles in the anterior compartment. Moreover, when corrected for differences in body weight, neither the EDL nor TA muscle wet weights were significantly different between contralateral and age-matched control muscles, indicating that VML injury *per se* did not result in a hypertrophic response of the contralateral uninjured musculature (Table 1).

TA muscle histological alterations

The VML injury resulted in scarring at the wound site, as indicated by increased collagen deposition (Fig. 2). The scarred area and the area immediately adjacent to it contained disorganized muscle fibers. Within the remaining muscle tissue, at both the 2- and 4-month time points, active muscle regeneration and repair was evident, as indicated by the increased presence of centrally located nuclei within muscle fibers (Fig. 3A–3C). Muscle remodeling was also evident in the injured muscle postinjury, as indicated by the increased collagen deposition within the remaining tissue (Fig. 3D–3I).

In situ *TA muscle functional characteristics*

During pilot studies, we observed that 20% muscle defect resulted in an immediate loss of 38.3±1.6% of P_o. The goal of this study was to determine if the 20% defect induced a sustained functional deficit out to 4 months postinjury, thus indicating that the VML model reflected the endogenously irrecoverable nature of the human condition.[7] Towards this end, the VML injury resulted in a significantly diminished functional capacity at both the 2- and 4-month time points

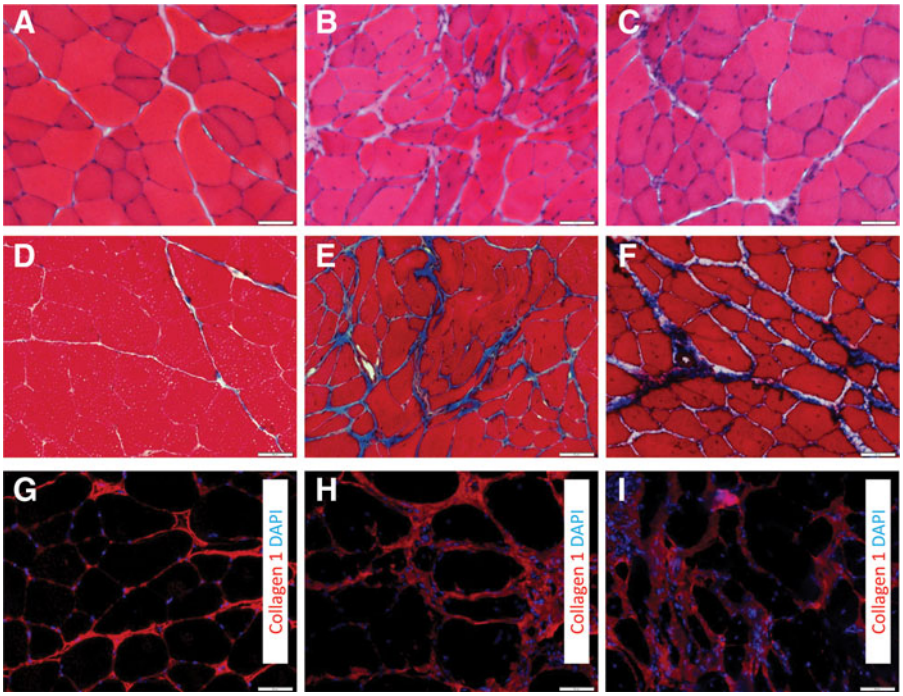

FIG. 3. Histological evidence of muscle fiber regeneration, fibrosis, and remodeling during the months after VML injury. Uninjured **(A, D, G)** and VML-injured muscles 2 months **(B, E, H)** and 4 months **(C, F, I)** postinjury were stained with hematoxylin and eosin (HE) **(A–C)**, Mason's Trichrome **(D–F)**, or collagen I (nuclei with DAPI) **(G–I)**. Cross sections were obtained from the area corresponding to the middle of the injury. Scale bar = 50 μm.

(Fig. 4; Table 1). TA muscles with VML produced 28.2% and 32.8% less force than contralateral muscles at 2 and 4 months, respectively. However, when P_o was normalized to muscle weight the differences between VML and the contralateral muscle were not different ($p > 0.05$). As with P_o, VML resulted in significantly less force at all submaximal stimulation frequencies when compared to the contralateral control TA (Fig. 4). However, when the force was expressed relative to P_o, the force-frequency curves were similar between VML and contralateral TAs, suggesting that Ca^{2+} handling within the remaining muscle fibers was not altered. Lastly, VML did not significantly impact the functional capacity of contralateral control TA muscles because P_o was similar between contralateral and age-matched muscles (Table 1). P_o normalized to body weight was similar between these groups, confirming the validity of using either the contralateral muscle or a separate age-matched rat as an uninjured control.

In vivo *anterior crural muscle functional assessment*

In vivo muscle function assessments allow for muscles to be tested under anatomical constraints and within physiological conditions, making this assessment advantageous for the study of VML. However, hypertrophy of the EDL muscle in response to VML injury (Table 1) would be expected to result in a greater contribution of the EDL muscle to anterior crural muscle net torque produced during dorsi flexion, which would mask the functional deficit of the TA muscle. To examine this possibility, we performed an experiment to determine peak isometric torque produced *in vivo* with and without the contribution of the EDL muscle by performing a tenotomy of the distal tendon in the injured and uninjured legs of each animal ($n = 4$) 4 months post-VML. In the uninjured leg, tenotomy of the EDL resulted in a 16.4% decline in P_o (N·mm/kg body weight) (Fig. 5). In contrast, elimination of the EDL in the VML injured leg resulted in a decline of 24.5%, indicating functional compensation of the EDL following TA VML injury. It is important to highlight that following distal EDL tenotomy (i.e., measurement of the TA in isolation), a 24.5% *in vivo* torque deficit was observed, which compares favorably to the 28.4% force deficit observed with *in situ* functional assessment.

Repair of VML with skeletal muscle-derived rat ECM

Most current tissue engineering strategies for VML repair involve the use of acellular scaffolds.[7,14–18,31] To demonstrate that the surgical model can serve as platform for testing current tissue engineering approaches, we performed an experiment in which VML was repaired with a RAMM scaffold. Both visual and microscopic examination showed that the RAMM was well integrated with the surrounding wound bed within 14 days after implantation (Fig. 6). As evidence, RAMM appeared to support a low level of muscle fiber regeneration near the interface of the remaining muscle tissue. Moreover, a significant degree of RAMM cellular infiltration was observed, with a portion of these cells staining positive for the general macrophage marker CD68. Lastly, there was significant vWF staining within the RAMM scaffold 2 weeks postinjury, suggesting that the scaffold had become revascularized. This observation was further supported by vital perfusion with India ink, indicating that by 2 weeks the RAMM had functional vascularization integrated with the host circulation. Overall, these results highlight that the VML model developed in these studies is appropriate for testing a variety of tissue engineering strategies for the treatment of VML.

Discussion

The present study describes a standardized, clinically relevant rodent model of VML injury. Here we have

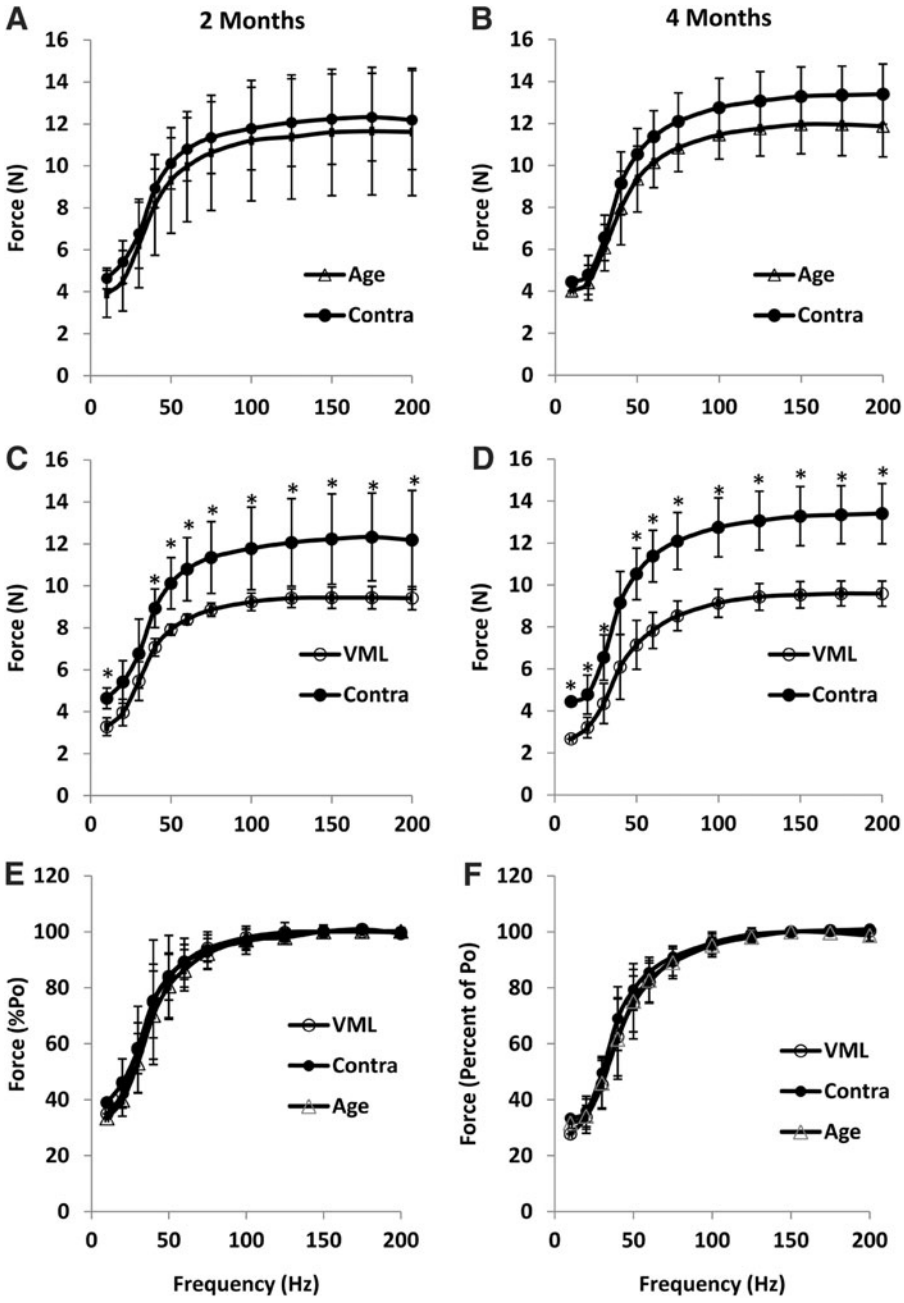

FIG. 4. The force–frequency relationships at 2 months **(A, C, E)** and 4 months **(B, D, F)**. Age-matched cage control (Age) and uninjured contralateral control (Contra) were compared with VML-injured subjects at 2 and 4 months. At both time points, isometric force was significantly less at most stimulation frequencies compared to Contra ($p > 0.05$). However, when force was expressed as percent of P_o **(E, F)**, there was no difference between groups at either time point. All values are mean ± standard deviation.

demonstrated that the injury (1) does not spontaneously heal, i.e., the injury results in a permanent loss of muscle function; (2) is technically easy to perform; (3) provides the ability to perform standard and reliable functional assessment; and (4) allows clinically relevant repair.

To create a standardized VML model, the rat TA muscle was selected as a platform because rat studies are relatively inexpensive, standard functional assessments of the anterior crural muscles (*in vivo*) or TA muscle (*in situ*) are developed, and per relative defect size (e.g., 20%) the absolute defect volume is at least 10 times greater in the rat than mouse TA muscle, offering a more clinically relevant injury. Since volumetric muscle loss is "The traumatic or surgical loss of skeletal muscle with resultant functional impairment",[1] it is imperative that the VML injury produced results in functional impairment in the form of a permanent loss of maximal tetanic force (P_o). With this model, the loss of P_o was approximately 30% at both 2 and 4 months postinjury (Fig. 4), as was determined by established *in situ* and *in vivo* functional procedures (Figs. 4, 5). A similar loss of submaximal isometric force was observed over the range of stimulation frequencies examined (Fig. 4). Moreover, the VML injury was reproducible, as attested to by the similar variability of P_o observed between uninjured and VML injured muscle. For example, the coefficient of variation, calculated as the ratio of one standard deviation to the group's mean (SD/mean), of P_o for uninjured and VML injured muscles was 0.06 and 0.04, respectively, at 2 months postinjury. That is, the rat TA muscle VML model developed here results in a sustained (i.e., 30% deficit at 4 months postinjury) and reliable (i.e., less than 5%

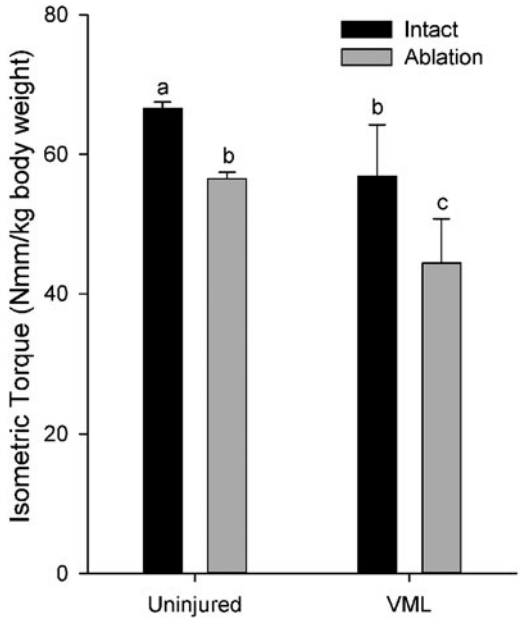

FIG. 5. *In vivo* isometric torque in the anterior crural muscles before (Intact) and after tenotomy of the extensor digitorum longus muscle (Ablation). [abc]Letters indicate that the value is significantly different from any different letter ($p < 0.05$).

variability at 2 months) functional deficit, despite multiple researchers performing the surgical procedures in this study. In summary, the data presented demonstrates the development of a standardized VML injury model suitable for testing tissue engineering therapies aimed at restoring function to traumatically injured skeletal muscle.

While tissue engineering solutions for VML are aimed at recapitulating presumptive *de novo* muscle fiber regeneration, it is important to also consider the muscle mass remaining following injury. It is clear from histological examination that active muscle degeneration and regeneration is still taking place in the general vicinity of the wound site as well as deep within the remaining musculature out to 4 months post-VML (Figs. 2, 3). The amount of connective tissue, and in particular type I collagen, within the remaining TA musculature also appears increased compared to uninjured muscle. Together these findings suggest that VML injury results in muscle fiber degeneration and regeneration in an effort to remodel the remaining musculature.

In the current model, VML resulted in significant compensatory hypertrophy of the EDL. That is, the initial loss of approximately 20% of TA muscle mass was associated with an approximate 15% and 17% increase in EDL muscle wet weight 2 and 4 months postinjury, respectively. This response is not unexpected because removal of the entire TA muscle has been shown to induce a corresponding approximate 20–25% increase in mass and P_o of the EDL muscle over a 1-month period.[32–34] One concern then is the interpretation of *in vivo* functional measures if the EDL muscle is left intact since the net torque reflects the compensatory hypertrophy of the EDL muscle (Fig. 5). For future studies with this VML model, researchers should measure the TA muscle force or torque *in situ* or *in vivo* in isolation, as presented in this study (Table 1; Figs. 4, 5). Alternatively, repeated *in vivo* functional assessments in the same rat could be performed reliably, as has been demonstrated in murine injury studies,[35–37] with further surgical manipulation (i.e., EDL ablation) at the time of injury, although consideration should be given to the increased load placed on the remaining VML injured TA muscle.

An important experimental design consideration with muscle injury models is the choice of an appropriate uninjured control muscle. Because various forms of muscle injury have been shown to significantly impact the uninjured, contralateral leg,[38] in this study age-matched cage control and uninjured contralateral muscle control groups were included to determine the suitability of each control for this VML injury model. At the beginning of the study, there was an ~6% difference in body weight between the age-matched cage control and VML injured groups; however, their magnitude of weight gain was nearly identical to that of the injured rats (e.g., from time 0 to 2 months the increase in weight was 31.4% and 34.6% for VML and age-matched cage controls, respectively.) When normalized to body weight, the age-matched controls and contralateral control muscle weights and mechanical properties were nearly identical when corrected for differences in body weight (Table 1; Fig. 4). Importantly, these findings indicate that VML did not impact the properties of the contralateral muscle; demonstrating that either a separate age-matched group or the contralateral control group may serve as an appropriate uninjured control for this model.

In addition to the objectives already discussed, we sought to develop a VML model that could be repaired using clinically relevant tissue engineering therapies. To date, there is only a single case report of surgical repair of VML involving a tissue engineering solution (i.e., a biological acellular scaffold)[7]; however, many current tissue engineering strategies for VML repair in preclinical studies involve the use of acellular scaffolds.[39,40] To this end, the VML model developed in this study was repaired with RAMM scaffold using simple surgical procedures similar to that currently used in a clinical application.[7] The RAMM did not dislocate from the area of implantation, integrated with the wound bed, and became well vascularized within 14 days of repair. Based on these findings, this VML model is appropriate as a testing platform for a variety of scaffold-based tissue engineering strategies.

VML models have previously been reported for the canine gastrocnemius/Achilles tendon,[17] rabbit lateral quadriceps,[41] rat lateral gastrocnemius (LG),[14] rat abdominus rectus,[16,42] murine TA muscles,[19,43] and murine tensor fasciae latae/rectus femoris.[20] All have strengths and weaknesses. For example, previously we developed a VML model in the LG muscle in the rat.[39,40] While the findings made with this model are reliable, it is a technically difficult model to perform. Surgically, creation of the LG-VML injury requires blunt dissection through the biceps femoris resulting in a secondary injury, and performing the repair is challenging. Functionally, the LG represents only one head of the gastrocnemius muscle (approximately 54% of the mass of the total gastrocnemius) and requires the medial and lateral portions of the gastrocnemius muscle to be separated, complicating *in situ* measurements of mechanical properties. Similarly, the rat abdominus rectus model is useful for testing solutions for abdominal hernia repair; however, the nature of its anatomy makes it difficult to use for meaningful functional measurements, i.e., the motor

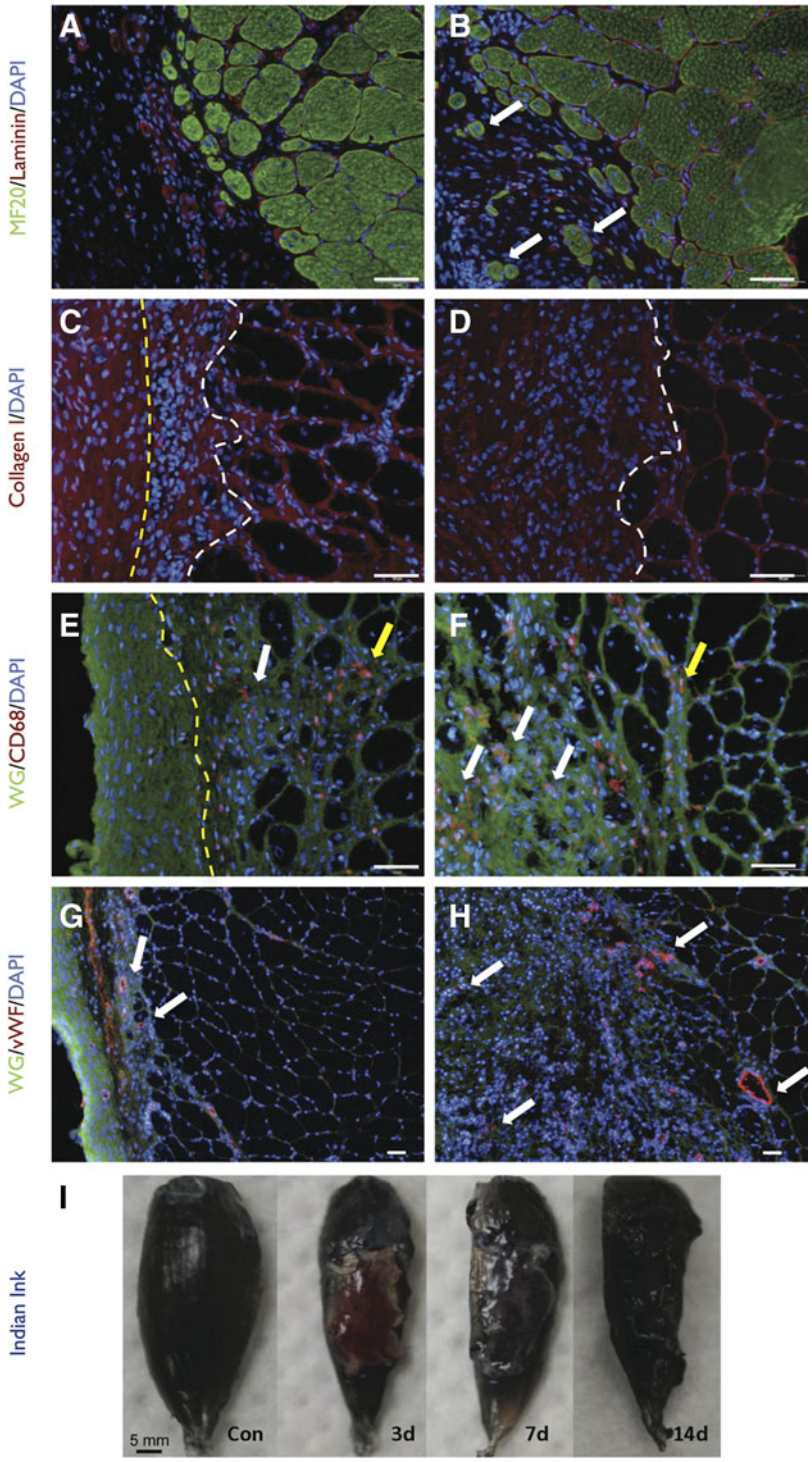

FIG. 6. Surgical repair of VML with muscle-derived rat extracellular matrix (RAMM). Unrepaired **(A, C, E, G)** and RAMM-repaired **(B, D, F, H)** TA muscles harvested 2 months after injury were analyzed using immunohistochemistry. **(A, B)** Regenerating myosin-positive muscle fibers (*white arrows*) in isolation from the remaining muscle mass were only observed in the defect area of RAMM-repaired muscles. **(C, D)** Collagen I deposition was prominent in the defect area of both unrepaired and RAMM-repaired muscle. However, the extent of collagen 1 deposition was qualitatively greater in RAMM-repaired muscle [area to left of *yellow line* is fascia, between lines is scar tissue, and to right of *white line* is muscle remaining muscle mass; no fascia is depicted in **(D)**]. **(E, F)** Macrophages (CD68) were present in the remaining muscle mass (*yellow arrows*) or in the area of collagen 1 deposition in the defect area (*white arrows*). The area to the left of the yellow line in E is fascia. **(G, H)** Vascularization (*white arrows*) in the defect area was detected using von Willebrand (vWF) staining. Nuclei were stained with DAPI. Stains are identified for each slide with color coded text in the left margin of each row; WG, wheat germ agglutinin. Scale bars = 50 μm. **(I)** Rats were perfused with Indian ink at 3, 7, or 14 days after implantation of RAMM to demonstrate an integrated vascular network with the host circulation.

nerve cannot be isolated, necessitating direct stimulation. The murine tensor fasciae latae/rectus femoris[20] can be used for rapid screening but does not lend itself to meaningful functional measurements. Lastly, canine models are attractive because the size of the muscle gives it clinical significance, but this animal model is prohibitively expensive to perform most preclinical studies with an appropriate sample size and duration required to adequately characterize a treatment. Further compounding the need for a standard preclinical VML injury model is that it is not possible to compare functional outcomes among these models, hindering the development of viable treatment solutions for VML injury.

In conclusion, we have presented a rat model that provides a useful platform for testing and developing tissue engineering and regenerative medicine approaches to the treatment of VML. Furthermore, we suggest the technical simplicity, reliability, and clinical relevance of the model make it ideal as a standard model for this purpose. The use of a standard model would facilitate comparison of results within and between laboratories working in developing solutions for VML.

Acknowledgments

The authors wish to express their gratitude to Ms. Janet L. Roe and Ms. Melissa Sanchez of the U.S. Army Institute of Surgical Research for their invaluable technical support. This research is supported by The U.S. Army Medical Research and Materiel Command-grant F_013_2010_USAISR and W81XWH-09-2-0177 to T.J.W.

Author Disclosure Statement

No competing financial interests exist. The opinions or assertions contained herein are the private views of the authors and are not to be construed as official or reflecting the views of the Department of Defense or the United States Government. The authors are employees of the U.S. government and this work was prepared as part of their official duties.

References

1. Grogan BF, Hsu JR. Volumetric muscle loss. J Am Acad Orthop Surg. 2011;19(Suppl. 1):S35–37.
2. MacKenzie EJ, Bosse MJ, Kellam JF, et al. Characterization of patients with high-energy lower extremity trauma. J Orthop Trauma. 2000;14:455–466.
3. Grogan B, Hsu JR. Volumetric muscle loss. J Am Acad Orthop Surg. 2011;19(Suppl. 1):S35–S39.
4. Owens BD, Kragh JF Jr, Wenke JC, et al. Combat wounds in operation Iraqi Freedom and operation Enduring Freedom. J Trauma. 2008;64:295–299.
5. Lew TA, Walker JA, Wenke JC, et al. Characterization of craniomaxillofacial battle injuries sustained by United States service members in the current conflicts of Iraq and Afghanistan. J Oral Maxillofac Surg. 2010;68:3–7.
6. Gassner R, Tuli T, Hachl O, et al. Cranio-maxillofacial trauma: a 10 year review of 9,543 cases with 21,067 injuries. J Craniomaxillofac Surg. 2003;31:51–61.
7. Mase VJ Jr, Hsu JR, Wolf SE, et al. Clinical application of an acellular biologic scaffold for surgical repair of a large, traumatic quadriceps femoris muscle defect. Orthopedics. 2010; 33:511.
8. Greene TL, Beatty ME. Soft tissue coverage for lower-extremity trauma: current practice and techniques. A review. J Orthop Trauma. 1988;2:158–173.
9. Fan C, Jiang P, Fu L, et al. Functional reconstruction of traumatic loss of flexors in forearm with gastrocnemius myocutaneous flap transfer. Microsurgery. 2008;28:71–75.
10. Vekris MD, Beris AE, Lykissas MG, et al. Restoration of elbow function in severe brachial plexus paralysis via muscle transfers. Injury. 2008;39(Suppl. 3):S15–22.
11. Lin CH, Lin YT, Yeh JT, Chen CT. Free functioning muscle transfer for lower extremity posttraumatic composite structure and functional defect. Plast Reconstr Surg. 2007;119: 2118–2126.
12. Owens JG, Blair JA, Patzkowski JC, et al. Return to running and sports participation after limb salvage. J Trauma. 2011; 71(Suppl. 1):S120–124.
13. Patzkowski JC, Blanck RV, Owens JG, et al. Can an ankle-foot orthosis change hearts and minds? J Surg Orthop Adv. 2011;20:8–18.
14. Merritt EK, Cannon MV, Hammers DW, et al. Repair of traumatic skeletal muscle injury with bone marrow derived mesenchymal stem cells seeded on extracellular matrix. Tissue Eng Part A. 2010;16:2871–2881.
15. Merritt EK, Hammers DW, Tierney M, et al. Functional assessment of skeletal muscle regeneration utilizing homologous extracellular matrix as scaffolding. Tissue Eng Part A. 2010;16:1395–1405.
16. Valentin JE, Turner NJ, Gilbert TW, Badylak SF. Functional skeletal muscle formation with a biologic scaffold. Biomaterials. 2010;31:7475–7484.
17. Turner NJ, Yates AJ Jr, Weber DJ, et al. Xenogeneic extracellular matrix as an inductive scaffold for regeneration of a functioning musculotendinous junction. Tissue Eng Part A. 2010;16:3309–3317.
18. Machingal MA, Corona BT, Walters TJ, et al. A tissue-engineered muscle repair construct for functional restoration of an irrecoverable muscle injury in a murine model. Tissue Eng Part A. 2011;17:2291–2303.
19. Rossi CA, Flaibani M, Blaauw B, et al. In vivo tissue engineering of functional skeletal muscle by freshly isolated satellite cells embedded in a photopolymerizable hydrogel. FASEB J. 2011;25:2296–2304.
20. Sicari BM, Agrawal V, Siu BF, et al. A murine model of volumetric muscle loss and a regenerative medicine approach for tissue replacement. Tissue Eng Part A. 2012;18: 1941–1948.
21. Willett NJ, Li MT, Uhrig BA, et al. Attenuated rhBMP-2 mediated bone regeneration in a rat model of composite bone and muscle injury. Tissue Eng Part C Methods. 2012 Nov 2 [Epub ahead of print]; DOI: 10.1089/ten.tec.2012.0290.
22. Ingalls CP, Warren GL, Armstrong RB. Dissociation of force production from MHC and actin contents in muscles injured by eccentric contractions. J Muscle Res Cell Motil. 1998;19: 215–224.
23. Plant DR, Beitzel F, Lynch GS. Length-tension relationships are altered in regenerating muscles of the rat after bupivacaine injection. J Appl Physiol. 2005;98:1998–2003.
24. Warren GL, Hulderman T, Mishra D, et al. Chemokine receptor CCR2 involvement in skeletal muscle regeneration. FASEB J. 2005;19:413–415.
25. Kragh JF Jr, Svoboda SJ, Wenke JC, et al. Suturing of lacerations of skeletal muscle. J Bone Joint Surg Br. 2005;87:1303–1305.
26. Wu X, Wolf SE, Walters TJ. Muscle contractile properties in severely burned rats. Burns. 2010;36:905–911.
27. Wu X, Baer LA, Wolf SE, et al. The impact of muscle disuse on muscle atrophy in severely burned rats. J Surg Res. 2010;164:e243–251.
28. Ashton-Miller JA, He Y, Kadhiresan VA, et al. An apparatus to measure in vivo biomechanical behavior of dorsi- and plantarflexors of mouse ankle. J Appl Physiol. 1992;72: 1205–1211.
29. Chiu CS, Weber H, Adamski S, et al. Non-invasive muscle contraction assay to study rodent models of sarcopenia. BMC Musculoskelet Disord. 2011;12:246.
30. Stern MM, Myers RL, Hammam N, et al. The influence of extracellular matrix derived from skeletal muscle tissue on the proliferation and differentiation of myogenic progenitor cells ex vivo. Biomaterials. 2009;30:2393–2399.
31. Corona BT, Machingal MA, Criswell T, et al. Further development of a tissue engineered muscle repair construct in vitro for enhanced functional recovery following implantation in vivo in a murine model of volumetric muscle loss injury. Tissue Eng Part A. 2012;18:1213–1228.
32. Freeman PL, Luff AR. Contractile properties of hindlimb muscles in rat during surgical overload. Am J Physiol. 1982; 242:C259–264.

33. Rosenblatt JD, Parry DJ. Gamma irradiation prevents compensatory hypertrophy of overloaded mouse extensor digitorum longus muscle. J Appl Physiol. 1992;73:2538–2543.
34. Rosenblatt JD, Yong D, Parry DJ. Satellite cell activity is required for hypertrophy of overloaded adult rat muscle. Muscle Nerve. 1994;17:608–613.
35. Corona BT, Balog EM, Doyle JA, et al. Junctophilin damage contributes to early strength deficits and EC coupling failure after eccentric contractions. Am J Physiol Cell Physiol. 2010;298:C365–376.
36. Ingalls CP, Wenke JC, Nofal T, Armstrong RB. Adaptation to lengthening contraction-induced injury in mouse muscle. J Appl Physiol. 2004;97:1067–1076.
37. Ingalls CP, Warren GL, Williams JH, et al. E-C coupling failure in mouse EDL muscle after in vivo eccentric contractions. J Appl Physiol. 1998;85:58–67.
38. Lu DX, Käser L, Müntener M. Experimental changes to limb muscles elicit contralateral reactions: the problem of controls. J Exp Biol. 1999;202:1691–1700.
39. Merritt EK, Hammers DW, Tierney M, et al. Functional assessment of skeletal muscle regeneration utilizing homologous extracellular matrix as scaffolding. Tissue Eng Part A. 2010;16:1395–1405.
40. Merritt EK, Cannon MV, Hammers DW, et al. Repair of traumatic skeletal muscle injury with bone-marrow-derived mesenchymal stem cells seeded on extracellular matrix. Tissue Eng Part A. 2010;16:2871–2881.
41. Kin S, Hagiwara A, Nakase Y, et al. Regeneration of skeletal muscle using in situ tissue engineering on an acellular collagen sponge scaffold in a rabbit model. Asaio J. 2007;53:506–513.
42. Jenkins SD, Klamer TW, Parteka JJ, Condon RE. A comparison of prosthetic materials used to repair abdominal wall defects. Surgery. 1983;94:392–398.
43. Boldrin L, Elvassore N, Malerba A, et al. Satellite cells delivered by micro-patterned scaffolds: a new strategy for cell transplantation in muscle diseases. Tissue Eng. 2007;13:253–262.

Address correspondence to:
Thomas J. Walters, PhD
United States Army Institute of Surgical Research
BHT1, Bldg 3611, Rm 289-3
3698 Chambers Pass
Fort Sam Houston, TX 78234-6315

E-mail: thomas.walters@us.army.mil